Original Article

JCBFM

Journal of Cerebral Blood Flow & Metabolism
2020, Vol. 40(4) 808–822

DOI: 10.1177/0271678X19845934
journals.sagepub.com/home/jcbfm
SAGE

Neurovascular coupling during optogenetic functional activation: Local and remote stimulus-response characteristics, and uncoupling by spreading depression

Maximilian Böhm[1,2], David Y Chung[1,3], Carlos A Gómez[4], Tao Qin[1], Tsubasa Takizawa[1,5], Homa Sadeghian[1], Kazutaka Sugimoto[1,6], Sava Sakadžić[4], Mohammad A Yaseen[4] and Cenk Ayata[1,7]

Abstract

Neurovascular coupling is a fundamental response that links activity to perfusion. Traditional paradigms of neurovascular coupling utilize somatosensory stimulation to activate the primary sensory cortex through subcortical relays. Therefore, examination of neurovascular coupling in disease models can be confounded if the disease process affects these multisynaptic pathways. Optogenetic stimulation is an alternative to directly activate neurons, bypassing the subcortical relays. We employed minimally invasive optogenetic cortical activation through intact skull in Thy1-channelrhodopsin-2 transgenic mice, examined the blood flow changes using laser speckle imaging, and related these to evoked electrophysiological activity. Our data show that optogenetic activation of barrel cortex triggers intensity- and frequency-dependent hyperemia both locally within the barrel cortex (>50% CBF increase), and remotely within the ipsilateral motor cortex (>30% CBF increase). Intriguingly, activation of the barrel cortex causes a small (~10%) but reproducible hypoperfusion within the contralateral barrel cortex, electrophysiologically linked to transhemispheric inhibition. Cortical spreading depression, known to cause neurovascular uncoupling, diminishes optogenetic hyperemia by more than 50% for up to an hour despite rapid recovery of evoked electrophysiological activity, recapitulating a unique feature of physiological neurovascular coupling. Altogether, these data establish a minimally invasive paradigm to investigate neurovascular coupling for longitudinal characterization of cerebrovascular pathologies.

Keywords

Evoked potentials, functional hyperemia, laser speckle imaging, neurovascular coupling, whisker barrel cortex

Received 1 November 2018; Accepted 1 March 2019

Introduction

Neurovascular coupling is a ubiquitous cerebrovascular response modulating regional cerebral blood flow

[1]Neurovascular Research Laboratory, Department of Radiology, Massachusetts General Hospital, Harvard Medical School, Charlestown, MA, USA
[2]Department of Neurology, Charité – Universitätsmedizin Berlin, Berlin, Germany
[3]Neurocritical Care and Emergency Neurology, Department of Neurology, Massachusetts General Hospital, Harvard Medical School, Boston, MA, USA
[4]Athinoula A. Martinos Center for Biomedical Imaging, Department of Radiology, Massachusetts General Hospital, Harvard Medical School, Charlestown, MA, USA
[5]Department of Neurology, Keio University School of Medicine, Tokyo, Japan
[6]Department of Neurosurgery, Yamaguchi University School of Medicine, Ube, Japan
[7]Stroke Service, Department of Neurology, Massachusetts General Hospital, Harvard Medical School, Boston, MA, USA

Corresponding author:
Cenk Ayata, Massachusetts General Hospital, 149 13th Street, 6403, Charlestown, MA 02129, USA.
Email: cayata@mgh.harvard.edu

(CBF) driven by neural activity within the same region. Neurovascular uncoupling is believed to be detrimental to tissue homeostasis, and may lead to or aggravate tissue injury or degeneration in the long term. Neurovascular uncoupling has been demonstrated in cerebrovascular diseases such as subarachnoid hemorrhage, ischemic stroke, traumatic brain injury, Alzheimer's disease, cerebral amyloid angiopathy and cerebral autosomal dominant arteriopathy, subcortical infarcts and leukoencephalopathy (CADASIL).[1–6] Therefore, physiological mechanisms and mediators of neurovascular coupling have been under intense investigation for more than a decade.[7]

Methods to examine neurovascular coupling often rely upon peripheral somatosensory stimulation to evoke cortical neural activity, recruiting subcortical relay centers from the spinal cord to brain stem, thalamus and cortex. Unfortunately, numerous factors can diminish the fidelity of this polysynaptic pathway, such as injury during invasive preparations, systemic physiology (e.g. blood chemistry, anesthesia), and the primary disease process in which neurovascular coupling is examined (e.g. cerebral ischemia, trauma, hemorrhage, or transgenic models of white matter degeneration such as CADASIL).[4,5] Therefore, a minimally invasive method that does not rely upon subcortical neurotransmission to evoke physiological cortical activation and neurovascular coupling has significant advantages.

The emergence of optogenetics has recently provided an alternative and minimally invasive method to activate select neuronal populations using precisely controlled light exposure. We have recently shown that optogenetic cortical activation can be employed in a minimally invasive fashion through intact skull to trigger cortical spreading depression (CSD).[8] Optogenetic stimulation has been used to evoke hemodynamic responses as well,[9–13] suggesting that some form of neurovascular coupling indeed occurs when neurons are activated optogenetically. However, whether the neurovascular coupling during optogenetic activation is analogous to somatosensory activation and its determinants are unknown. We, therefore, aimed to develop the hyperemic response to optogenetic functional activation as a minimally invasive model system to be implemented in injured brain (hemorrhage, ischemia, trauma) to interrogate neurovascular coupling. As part of this aim, we sought evidence for mechanistic overlap with neurovascular coupling during physiological (e.g. somatosensory) functional activation. Using transgenic mice expressing the light-activated non-selective cation channel channelrhodopsin-2 (ChR2) under the control of the Thy1 promoter,[14,15] we undertook a detailed examination of the relationship between optogenetic stimulus parameters and local and remote cortical responses using full field laser speckle imaging of CBF coupled to evoked electrophysiological activity. Our data reveal intensity- and frequency-dependent functional hyperemia within the activated region, and complex hyperemic and oligemic responses in distinctly remote cortical regions, reflecting excitatory and inhibitory connectivity. Moreover, we provide evidence that the local and remote optogenetic CBF responses are susceptible to neurovascular uncoupling after CSD, just as physiological neurovascular coupling is known to be.

Methods

Animals

Experiments were approved by the MGH Institutional Animal Care and Use Committee, and carried out in accordance with the Guide for Care and Use of Laboratory Animals (NIH Publication No. 85-23, 1996). We used 12–32-week-old (84% of mice were 16–25 weeks old) male ChR2$^+$ ($n = 32$, homozygous line 18, (B6.Cg-Tg(Thy1-COP4/EYFP)18Gfng/J, Jackson Laboratories, Bar Harbor, ME, USA),[14,15] while C57BL/6 mice ($n = 17$; Charles River Laboratories, Wilmington, MA, USA) served as wild type controls (ChR2$^-$).

Anesthesia and surgical preparation

Mice were anesthetized with isoflurane (2.5% induction, 1% maintenance in 70%N_2/30%O_2). A femoral artery catheter was used to monitor arterial blood pressure, pH, pO_2, pCO_2 (Table 1). Periods with mean arterial blood pressure $\leq$60 mmHg were excluded from analysis. Rectal temperature was monitored and maintained at 37 °C via a servo-controlled heating pad. Animals were placed in a stereotaxic frame. After a midline scalp incision and retraction, the skull surface was covered with a thin layer of mineral oil to prevent

Table 1. Systemic physiological parameters.

	ChR2$^+$		ChR2$^-$	
	Start	End	Start	End
MABP (mmHg)	74 ± 8	68 ± 11	78 ± 8	79 ± 9
pH	7.40 ± 0.04	7.37 ± 0.04	7.40 ± 0.01	7.38 ± 0.01
pO_2 (mmHg)	133 ± 17	138 ± 20	131 ± 14	122 ± 26
pCO_2 (mmHg)	36 ± 4	40 ± 3	36 ± 2	40 ± 2

drying and an optical fiber was positioned over the medial whisker barrel cortex using a stereotaxic arm (3 mm lateral and 1 mm posterior to bregma) for optogenetic stimulation. After surgical preparation, mice were injected with 300 mg/kg chloral hydrate intraperitoneally, and isoflurane was weaned off over 10 min. Experiments started 10 min after isoflurane was completely off. A maintenance dose of chloral hydrate (100 mg/kg) was given every 45 min, or sooner if the animal showed signs of awakening.

Optogenetic stimulation

We chose the whisker barrel cortex to apply optogenetic stimulation because this is the most frequently studied region to examine neurovascular coupling. The light stimulus was applied through a 400-μm diameter fiber (Numerical aperture 0.39) using a 470 nm LED light source (LED: MF470F3; LED driver: DC2100; Thorlabs, Newton, NJ, USA) controlled by the computer and analog-digital converter (PowerLab, ADInstruments, Colorado Springs, CO, USA). Power was calibrated before each experiment using a power meter (PM16-130, Thorlabs). Optogenetic stimuli were delivered either as 30-s train stimulation at various intensities (1–5 mW), frequencies (4–12 Hz) and pulse durations (2–10 ms) to evoke a CBF response, or as single pulses at various intensities (1–5 mW) and pulse durations (2–10 ms) to evoke field potentials. Stimulation paradigms for each dataset are shown on the figures and detailed in figure legends.

Laser speckle flowmetry

Cortical blood flow (CBF) was imaged through intact skull by laser speckle flowmetry (LSF) using a near-infrared laser diode (785 nm, 75 mW) and a CCD camera (CoolSnap *cf*, 1392 × 1040 pixels; Photometrics, Tucson, AZ), as described previously.[16] Raw speckle frames were acquired at 17 Hz and speckle contrast frames averaged, to yield a CBF image every 3.5 s. The experimental setup allowed precise placement of the optogenetic stimulus and provided a full field view of regional CBF changes throughout the dorsal cortex. CBF changes were analyzed in three ipsilateral and corresponding contralateral regions of interest (ROIs), each with a diameter of approximately 1.5 mm and centered around the following coordinates relative to bregma: (1) 2 mm anterior and 2 mm lateral (motor cortex), (2) 1 mm posterior and 3 mm lateral (whisker barrel cortex), and (3) 3.5 mm posterior and 2.5 mm lateral (visual cortex) according to the Paxinos and Franklin mouse brain atlas.[17] Large pial vessels and skull opacities were avoided when defining the ROIs. The centers of ROIs placed over motor and visual cortices were approximately equidistant from the optogenetic light source placed over the whisker barrel cortex (3.01 ± 0.14 and 3.05 ± 0.18 mm, respectively). We imaged CBF at baseline (30 s), during optogenetic stimulation (30 s), and after the end of stimulation (90 s), and expressed it relative to baseline. Since CBF is in part dependent on sudden systemic blood pressure changes, we also calculated cerebrovascular resistance (CVR) by dividing the average systemic arterial blood pressure during the acquisition of each image by the relative CBF value calculated for that image, and expressed it also as percentage of baseline CVR, as previously described.[3]

Optogenetic and somatosensory evoked potentials

To record evoked field potentials, animals received the same surgical preparation as for the CBF study, with the exception of arterial catheterization to allow longer experimental recordings by minimizing invasive surgery. Single light pulses (1, 3 or 5 mW, and 2, 6 or 10 ms) were applied every 5 s through the optical fiber placed over the whisker barrel cortex. Epicranial evoked potentials were recorded consecutively over six ROIs with a ball electrode in contact with intact skull via conducting gel at the same coordinates as for the CBF study, using an amplifier (Axoprobe 1A, Axon Instruments, Molecular Devices, San Jose, CA, USA) and digitized for offline analysis (Scope, ADInstruments, Colorado Springs, MO, USA). For each stimulus level, 20 evoked potentials were averaged. For somatosensory evoked potentials (SSEP), an electrical stimulus (3 mA, 1 ms) was delivered to the ipsilateral whisker pad via subcutaneous electrodes, and evoked potentials were recorded over the contralateral whisker barrel cortex as described above (12 sweeps, 0.2 Hz). To test transhemispheric inhibition, contralateral whisker pad was stimulated as above simultaneously with optogenetic transcallosal stimulation of the contralateral whisker barrel cortex (3 mW, 6 ms, 4 or 12 Hz).

CSD induction and detection

CSD was induced optogenetically through intact skull over the ipsilateral whisker barrel cortex with a 10 s continuous light stimulus with an intensity of 3 mW, as recently described.[8] LSF was used to both detect CSD and record CBF changes during optogenetic activation as described above. Optogenetic EPs were recorded before, during and for 60 min after the CSD using two ball electrodes placed over the ipsilateral whisker barrel and motor cortices simultaneously (12 sweeps, 0.2 Hz).

Cortical temperature measurement

In a separate group of mice, we measured brain temperature during light stimulation at the highest power,

duration and frequency using a BAT-12/IT-23 thermocouple microprobe thermometer (Physitemp, Clifton, NJ, USA) inserted through a burr hole. The tip of the thermometer was placed below the skull surface right under the light source.

Design and statistical analysis

Study design and reporting followed ARRIVE guidelines. Data are presented as mean ± standard deviation. Statistical comparisons were made using one- or two-way repeated-measures ANOVA, Kruskal–Wallis, and paired *t*-test as appropriate (Prism 6, GraphPad Software, Inc., CA, USA), and indicated for each data set in figure legends. Sample sizes were selected empirically to achieve 80% power to detect 50% effect size with an estimated coefficient of variation of 30% (α=0.05), and are indicated in the text and on the figures where relevant. In the absence of an intervention, blinding was not applicable. *P* value less than 0.05 was considered statistically significant.

Results

CBF responses

In wild-type mice without ChR2 expression ($ChR2^-$), light application did not cause any CBF change (Figure S1). In $ChR2^+$ mice, optogenetic stimulation led to distinct CBF changes within the stimulated region as well as the ipsilateral motor and contralateral whisker barrel cortices ($n = 8$ mice). In the stimulated (i.e. ipsilateral) whisker barrel cortex, hyperemia emerged within 3 s after stimulus onset, started to plateau during the stimulation, and peaked after the end of the 30-s stimulus (Figure 1). Thereafter, CBF gradually returned to normal within 1 min, without a consistent post-hyperemic dip. The magnitude of hyperemia was directly related to the intensity and the frequency of the stimulus, but not pulse duration (Figures 1 and 2). At the highest stimulus intensity or frequency, average hyperemia reached approximately 40% of baseline, and peak hyperemia was more than 50% of baseline (Figure 2). Optogenetic stimulus parameters did not significantly affect the shape of the hyperemic response. At the midrange of stimuli (3 mW pulse intensity, 8 Hz pulse frequency, 6 ms pulse duration), hyperemic response had a half-amplitude rise-time of ~7 s, and a half-amplitude decay-time of ~20 s.

Ipsilateral motor cortex, which receives strong projections from the barrel cortex,[18,19] also showed a large and spatially distinct hyperemic response (Figure 1, yellow arrow). Although its time course was similar to the stimulated ipsilateral whisker barrel cortex, hyperemia in motor cortex emerged a few seconds later (i.e. 1 frame, 3.5 s) than the whisker barrel cortex (Figure 1(d)); limited temporal resolution did not permit calculation of the lag between barrel and motor cortices with higher precision. The magnitude of hyperemia was directly related to pulse intensity and frequency, and to a lesser extent pulse duration (Figures 1 and 2). At the highest stimulus intensity, frequency or duration, average hyperemia in ipsilateral motor cortex was approximately 20% of baseline, while the peak hyperemia was more than 30% (Figures 1 and 2).

In contrast, contralateral whisker barrel cortex displayed a small but highly reproducible oligemic response during optogenetic stimulation. Oligemia troughed during the stimulus, rapidly resolved after stimulus cessation (Figure 1), and appeared to be strongest at the midrange of stimuli (Figure 2). The largest drop in CBF in contralateral whisker barrel cortex was approximately 10% of baseline. Visual cortices did not show consistent CBF changes during the stimulation, although at 6 Hz stimulus frequency (3 mW, 6 ms) there appeared to be a small oligemic response bilaterally (Figures 1 and 2). The absence of hyperemia in visual cortex also confirmed that the large hyperemic response in ipsilateral motor cortex was not due to direct contamination by optogenetic light applied over the barrel cortex, because the motor and the visual cortices were equidistant from the stimulation site over the barrel cortex. In the contralateral motor cortex, CBF changes did not reach statistical significance.

Last but not the least, to eliminate a potential confounding effect of systemic blood pressure changes on cortical CBF, we calculated changes in CVR during optogenetic neural activation, and reached identical conclusions as above (Figure 2).

Evoked potentials

To test whether CBF responses to optogenetic neural activation are linked to local electrical activity, we recorded cortical evoked potentials using epicranial electrodes. Optogenetic stimulation of ipsilateral whisker barrel cortex evoked morphologically distinct and highly reproducible transcranial field potentials in all six regions studied ($n = 5$ mice; Figure 3).

Over the stimulated whisker barrel cortex, light evoked an immediate negative potential shift that directly corresponded to the stimulus intensity (Figure 3, black arrowheads). This immediate negative shift was not observed in any other region, and therefore was presumably the local field generated directly by the activation of ChR2, as recently described.[8] A much larger negative field potential (N1) was superimposed on this early response. The evoked response over the ipsilateral motor area was biphasic with an initial positive (P1) followed by a negative (N1) potential shift. The latency

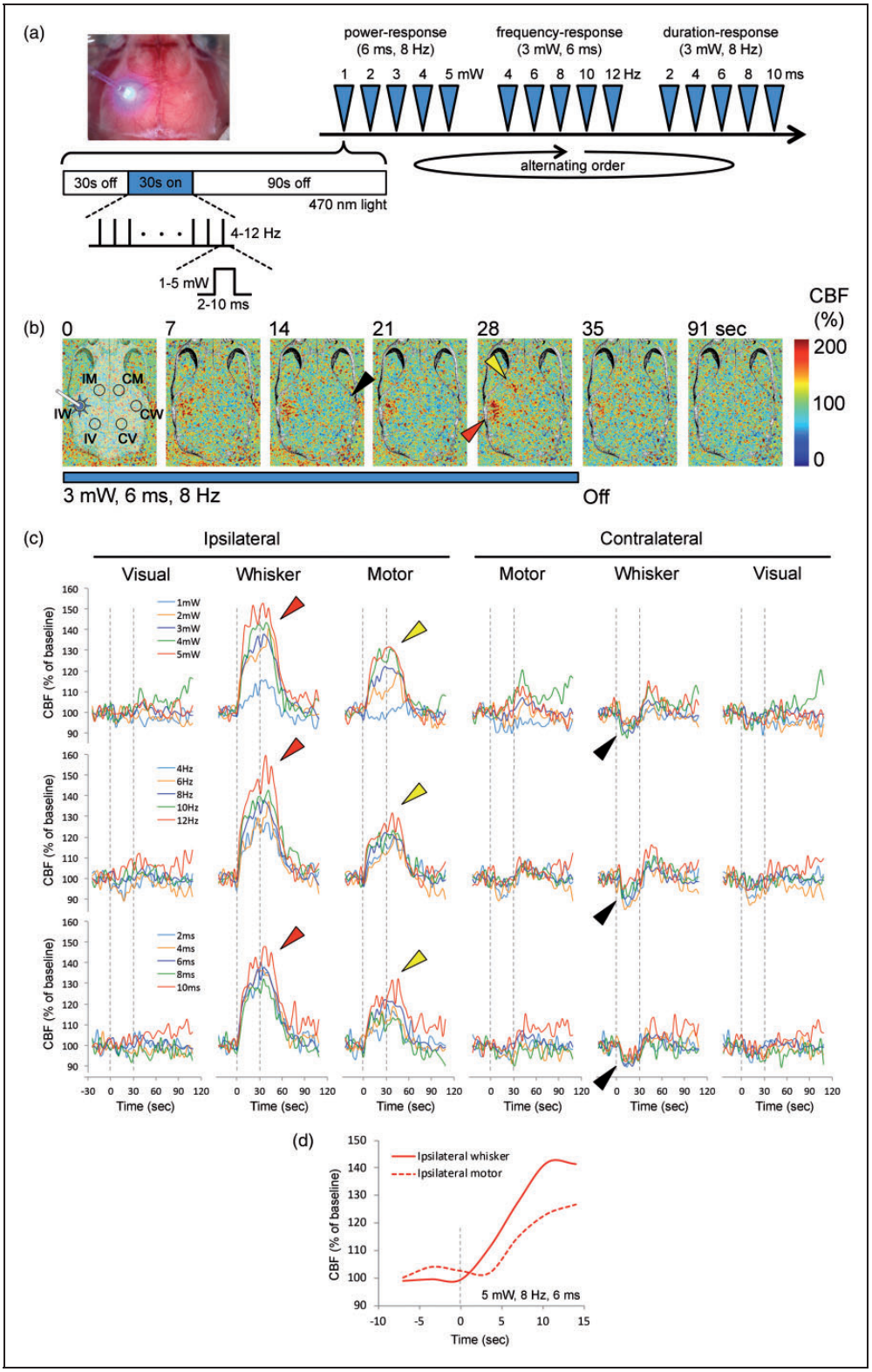

Figure 1. Local and remote regional CBF responses to optogenetic activation of barrel cortex. (a) Experimental setup and protocol: Upper left image shows a typical preparation for optogenetic stimulation and laser speckle CBF imaging through intact skull. The fiberoptic and 470 nm light are shown overlying the whisker barrel cortex. Timeline shows the stimulation protocol where power- (1–5 mW, 6 ms, 8 Hz), frequency- (4–12 Hz, 3 mW, 6 ms) and duration-response (2–10 ms, 3 mW, 8 Hz) trials were delivered in alternating order in different animals to control for any time effect. Each stimulus consisted of 30-s light off (baseline), 30-s light on

of motor N1 was twice that of whisker barrel N1. Contralateral whisker and motor areas also showed biphasic evoked potentials similar in morphology to those over the ipsilateral motor region, but with smaller peak amplitudes and longer peak latencies. Visual areas developed much smaller evoked potentials, which were monophasic negative over the ipsilateral visual cortex, and predominantly positive over the contralateral visual cortex. In most regions, the peak amplitudes of evoked potentials increased and the peak latencies decreased with increasing optogenetic pulse intensities (1–5 mW). In contrast, optogenetic pulse duration (2–10 ms) influenced the peak amplitudes much less than the pulse intensity did, and peak latencies were not shortened by increasing pulse durations (Figure S2). Lastly, in ChR2$^-$ mice, optogenetic light stimulation at the highest intensity did not evoke a potential shift in remote connected regions, and induced a very small ($\sim$0.1 mV) negative potential shift within the stimulated barrel cortex (Figure S1(c), *), the nature of which is unclear at this time.

Altogether, these data confirmed functional activation of local tissue and remote projection areas by optogenetic stimulation of barrel cortex, but revealed a dissociation between the amplitude and shape of the evoked potentials and the amplitude and polarity of the CBF response.

Transhemispheric inhibition

The intensity-dependence of ipsilateral barrel and motor evoked potentials and hyperemic responses was congruent. However, the large evoked potentials in contralateral barrel cortex, similar in shape to ipsilateral motor area, were rather surprising given the small but highly reproducible oligemic responses in this region. One potential explanation was that optogenetic transcallosal input to the contralateral barrel cortex exerted an inhibitory effect on local activity. To test this, we designed an experiment electrically stimulating the whisker pad to generate contralateral somatosensory evoked potentials (SSEP), and examined whether concurrent optogenetic stimulation of the ipsilateral whisker barrel cortex affects the whisker SSEPs ($n = 4$ mice; Figure 4). Stimulation of the whisker pad (3 mA, 1 ms current pulses at 0.2 Hz) generated large amplitude SSEPs over the contralateral barrel cortex. Concurrent optogenetic stimulation of the ipsilateral barrel cortex (3 mW, 6 ms, 4 or 12 Hz) significantly reduced the whisker pad SSEP amplitudes, confirming transcallosal inhibition between the barrel cortices, as reported previously.[20,21] These data explained the oligemic responses in contralateral barrel cortex during optogenetic stimulation.

Neurovascular uncoupling

Neurovascular coupling is a complex phenomenon with multiple potential mediators and mechanisms.[7,22,23] Although the hyperemic response in ipsilateral motor cortex was presumably induced by synaptic input from barrel cortex projections, and thus represents physiological neurovascular coupling, the local hyperemic response within the illuminated barrel cortex might be mediated by mechanisms unrelated to physiological neurovascular coupling. To address this, we examined whether the hyperemic response during optogenetic stimulation displayed features of physiological neurovascular coupling. CSD is an intense but brief (<1 min) neuronal and glial depolarization event that disrupts neurovascular coupling for more than an hour in otherwise normal brain tissue.[24] Therefore, we induced CSD unilaterally once again using optogenetic stimulation as described in detail recently,[8] and examined optogenetic hyperemic responses before and after CSD ($n = 5$ mice; Figure 5).

Prior to the CSD (i.e. baseline), optogenetic stimulation of the whisker barrel cortex (3 mW, 8 Hz, 6 ms) once again evoked hyperemic responses in both the ipsilateral barrel ($18.8 \pm 6.5\%$) and motor cortices ($10.0 \pm 6.0\%$; Figure 5), whereas contralateral regions developed a small oligemia (Figure S3). As expected, CSD caused a significant reduction in resting CBF

Figure 1. Continued
(train with specific parameters as indicated) and 90-s light off (recovery) periods, during which CBF was continuously imaged using laser speckle. (b) Representative time-lapse laser speckle images showing relative CBF changes (% of baseline) during 3 mW, 6 ms, 8 Hz optogenetic light stimulation (blue bar). The time is shown on upper left of each frame. The outline of skull, and the approximate regions of interest (IM, IW and IV, ipsilateral motor, whisker and visual cortices, CM, CW and CV, contralateral motor, whisker and visual cortices, respectively) within which CBF changes were quantified are also shown. Red arrowhead shows the regional CBF increase within the illuminated barrel cortex. Yellow arrowhead shows the regional CBF increase within the remotely activated ipsilateral motor cortex. Black arrowhead shows the small but highly consistent CBF reduction observed in the contralateral whisker barrel cortex. (c) Time course of CBF changes within the six regions of interest for escalating pulse power (1–5 mW, 6 ms, 8 Hz; upper row), pulse frequency (4–12 Hz, 3 mW, 6 ms; middle row) and pulse duration (2–10 ms, 3 mW, 8 Hz; lower row) trials. Dashed lines indicate light on and off. Arrowheads indicate flow changes as shown in (b). Each tracing is an average of $n = 8$ mice. Error bars were omitted for clarity. (d) CBF changes at the onset of stimulation show that the hyperemia in stimulated whisker barrel cortex started $\sim$5 s before ipsilateral motor cortex.

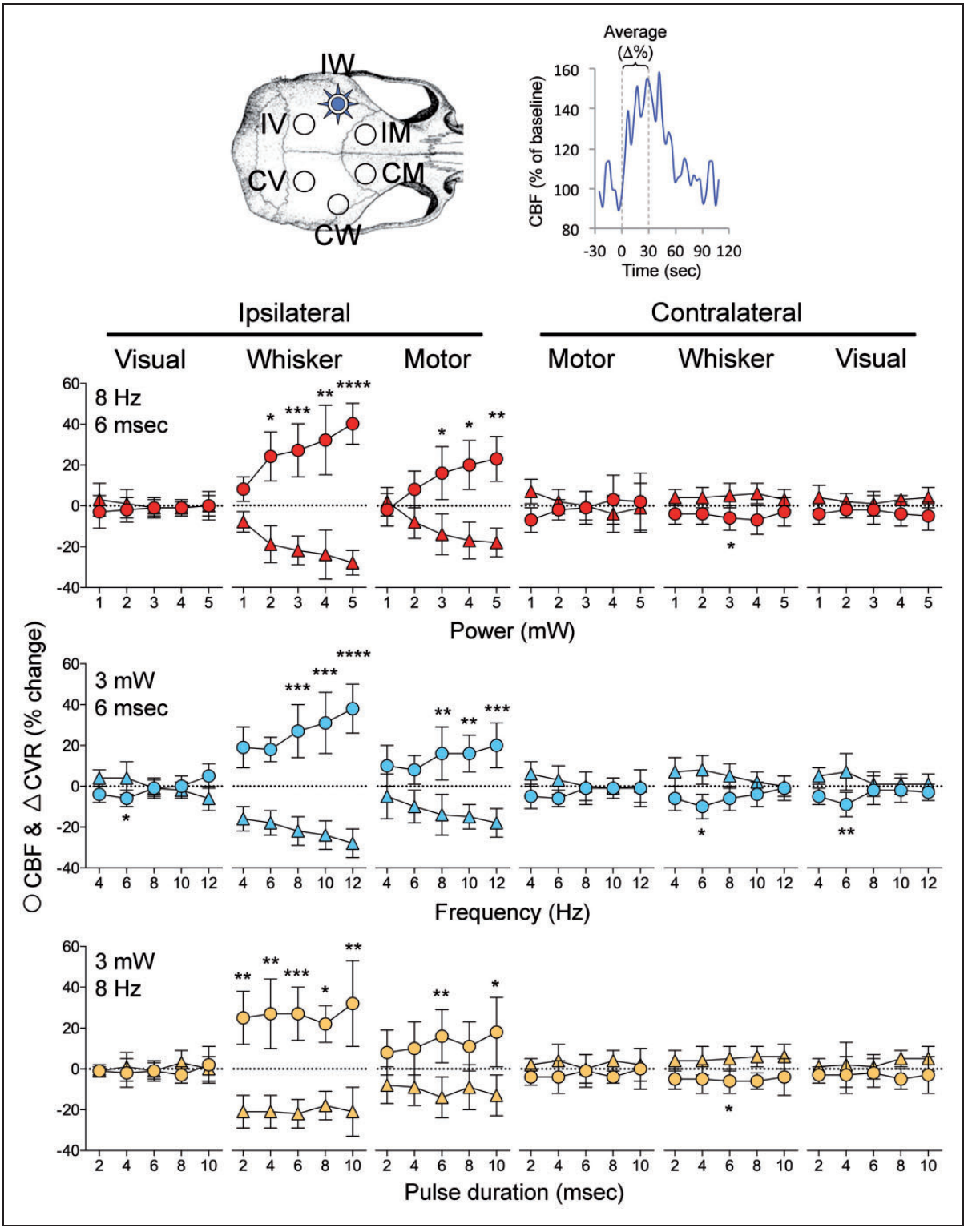

Figure 2. Effect of pulse intensity, frequency and duration on optogenetic CBF responses. Changes in CBF (circles) and CVR (triangles) in six regions of interest (upper left) were quantified by averaging the 30-s stimulation period (as shown in upper right). Graphs show the relationship between power (1–5 mW; 8 Hz, 6 ms), pulse frequency (4–12 Hz; 3 mW, 6 ms) or pulse duration (2–10 ms; 3 mW, 8 Hz), and the CBF and CVR responses calculated as percent change from baseline ($n = 8$ mice). *$p < 0.05$, **$p < 0.01$, ***$p < 0.001$, ****$p < 0.0001$ vs. baseline. One-way ANOVA for repeated measures followed by Dunn's multiple comparisons.

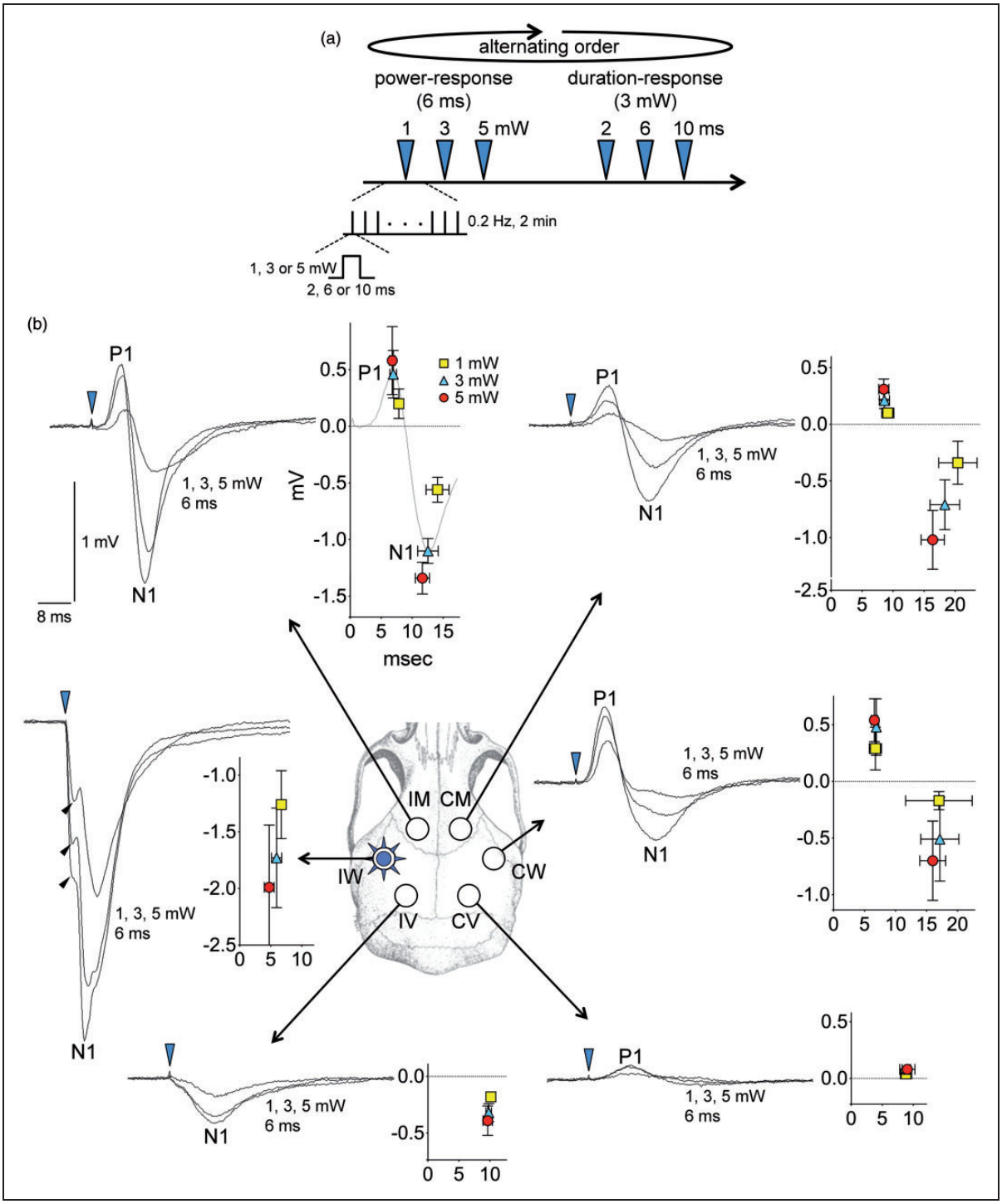

Figure 3. Optogenetic epicranial evoked potentials. (a) Timeline shows the stimulation protocol where escalating power (1, 3, 5 mW, 6 ms, 8 Hz) and duration (2, 6, 10 ms, 3 mW, 8 Hz) trials were delivered in alternating order in different animals to control for time effect. Each trial consisted of single light pulses of indicated intensity and duration delivered at 0.2 Hz for 2 min ($n = 24$), and evoked field potentials were averaged. (b) Epicranial evoked field potentials in response to 1, 3 or 5 mW light intensity (6 ms fixed duration) are shown for each of the six regions of interest (IM, IW and IV, ipsilateral motor, whisker and visual cortices, CM, CW and CV, contralateral motor, whisker and visual cortices, respectively). On the left of each panel for each region, representative tracings at each intensity level from one animal are shown superimposed. On the right of each panel for each region, averaged response amplitudes for positive and negative peaks (P1 and N1, respectively) are shown as indicated ($n = 5$ mice), along with standard for both the amplitude (mV) and the latency (ms) of the peaks (time 0 indicates optogenetic stimulus onset). Blue arrowhead shows the light stimulus onset. Black arrowheads indicate the direct negative potential shift associated with local light exposure in ipsilateral whisker barrel cortex (IW). The pulse duration–response relationship is shown in Supplemental Figure 2.

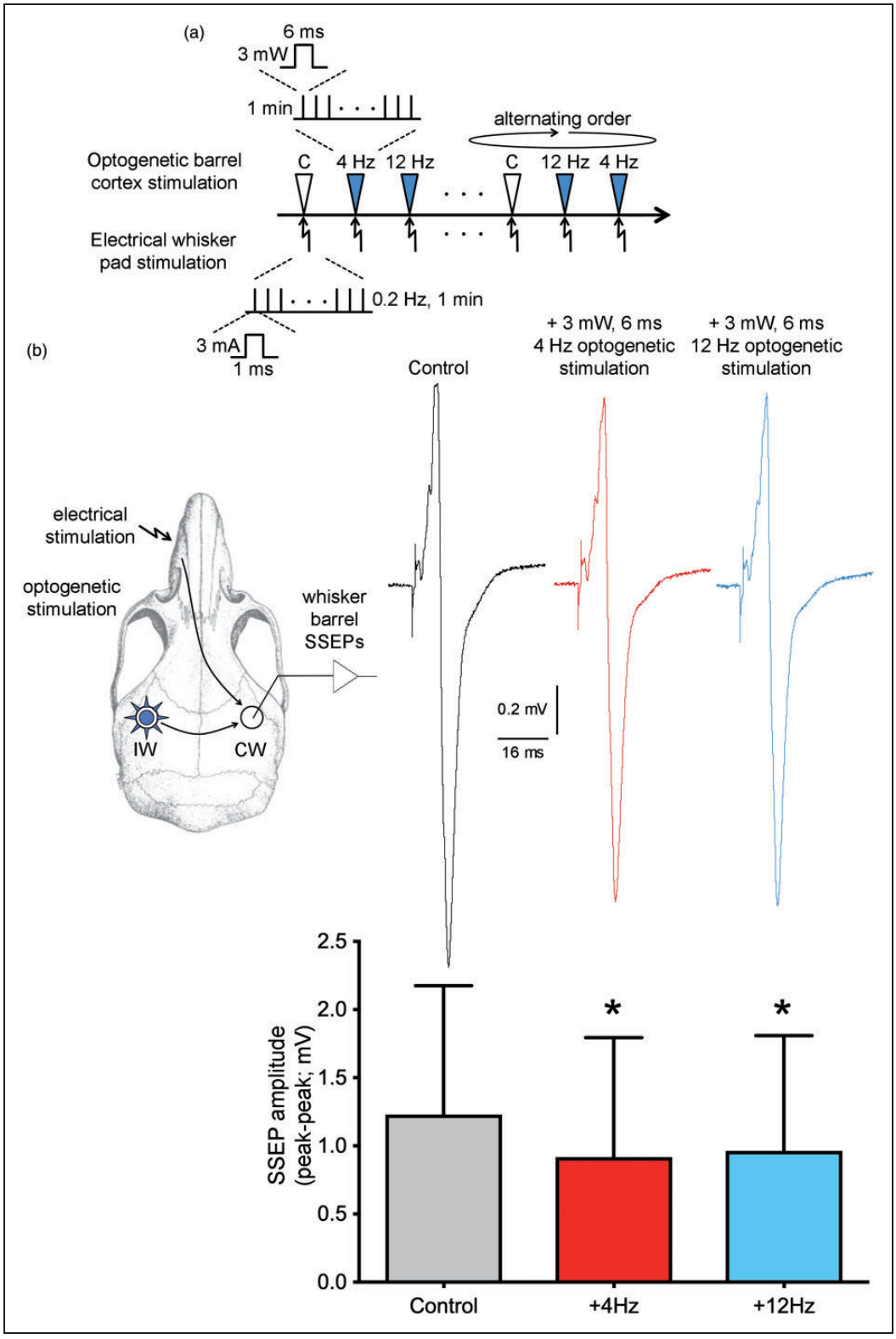

Figure 4. Concurrent optogenetic activation of whisker barrel cortex inhibits contralateral barrel cortex somatosensory evoked field potentials. (a) Timeline shows the stimulation protocol where optogenetic stimulation of whisker barrel cortex (3 mW, 4 or 12 Hz, 6 ms; arrowheads) was delivered in alternating order with controls (i.e. no optogenetic light) coincident with electrical stimulation of whisker pad (3 mA, 1 ms, 0.2 Hz; arrows) for 1 min. C: non-illuminated control. (b) Experimental design is shown on the left. Representative contralateral whisker barrel cortex somatosensory evoked potentials (SSEP) are shown on the right, averaged over 1 min without (Control) or with 4 Hz or 12 Hz optogenetic stimulation of the barrel cortex. Bar graph shows peak-to-peak SSEP amplitudes. Multiple trials within each animal were averaged for a single data point per animal ($n = 4$ mice). *$p < 0.05$ vs. Control; one-way ANOVA for repeated measures followed by Holm–Sidak's multiple comparisons.

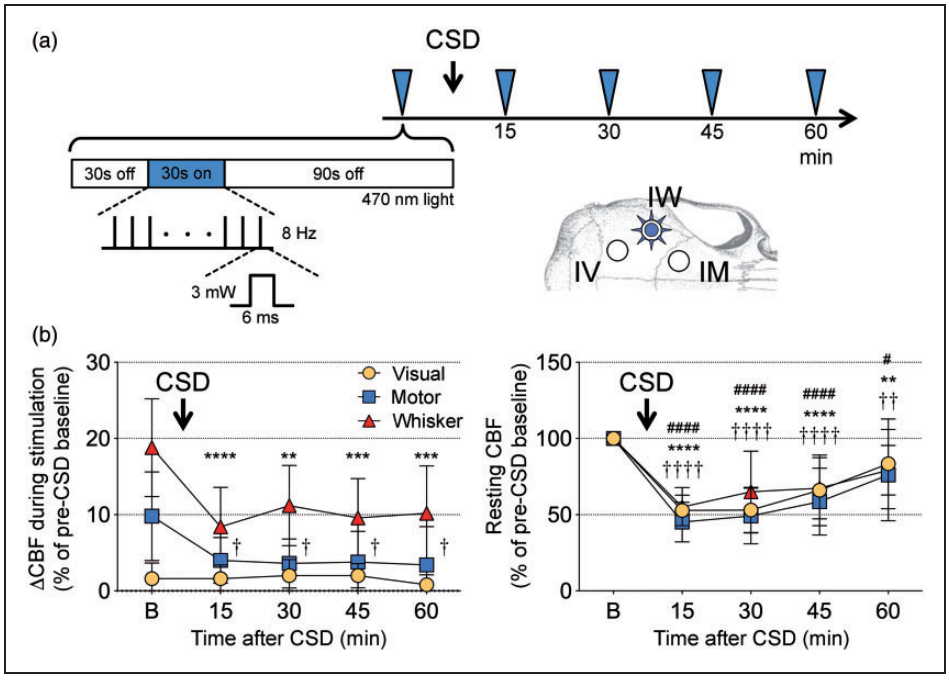

Figure 5. Effect of cortical spreading depression on optogenetic neurovascular coupling. (a) Timeline shows the stimulation protocol where optogenetic stimulation of whisker barrel cortex (3 mW, 8 Hz, 6 ms; blue arrowheads) was delivered every 15 min to evoke a CBF response in ipsilateral whisker, motor and visual cortices (IW, IM, IV, respectively) imaged during baseline (30 s light off), stimulation (30 sec light on), and recovery (90 s light off) using laser speckle flowmetry. A single cortical spreading depression (CSD) was induced using strong optogenetic activation (see Methods) immediately after the first stimulation. (b) Left panel shows the CBF response to optogenetic stimulation in the three regions of interest before (b) and 15–60 min after a CSD. Right panel shows resting CBF changes quantified using laser speckle imaging. The characteristic post-CSD oligemia lasted more than an hour in all three regions of interest. $p < 0.05$–0.0001 vs. baseline for whisker (*), motor (†), visual cortex (#; $n = 5$ mice). One-way ANOVA for repeated measures followed by Dunnett's multiple comparisons.

throughout the ipsilateral cortex (i.e. post-CSD oligemia) that slowly recovered over 60 min.[24] Interestingly, contralateral cortex also showed lasting CBF changes after CSD; while the whisker barrel cortex became progressively hyperemic, motor cortex developed mild oligemia that did not reach statistical significance (Figure S3). Induction of CSD diminished the optogenetic hyperemic responses by ~50%, not only in the illuminated cortex locally, but also in the ipsilateral motor cortex (Figure 5). Contralateral oligemic responses were also diminished (Figure S3). Despite the recovery of post-CSD oligemia at 60 min, neurovascular coupling during optogenetic activation remained disrupted (Figure 5).

More importantly, neural activation was only briefly disrupted by CSD ($n = 5$ mice; Figure 6). As expected, CSD immediately abolished all evoked activity. However, evoked potentials recovered within 2–4 min after CSD in both whisker barrel and motor cortices, and were indeed potentiated for at least 30 min, at a time when optogenetic functional hyperemia was still severely depressed in both regions. These data altogether confirmed that neurovascular coupling during optogenetic neural activation is disrupted by CSD, recapitulating a cardinal feature of neurovascular coupling during physiological neural activation.

Examination of potential confounders

We examined the possibility of inadvertent activation of ChR2 by ambient light. Room light did not significantly affect CBF in either the $ChR2^-$ or the $ChR2^+$ mice (Figure S4). In contrast, turning on the stereomicroscope light source (6.2 ± 0.8 mW, white light) increased CBF by 7% and 11%, in $ChR2^-$ and $ChR2^+$ mice, respectively ($p < 0.05$ vs. dark; $p > 0.05$ $ChR2^-$ vs. $ChR2^+$). Hence, all our experiments were carried out with room light on and surgical microscope light off. Lastly, optogenetic stimulation can raise tissue temperature.[8,25] We, therefore, measured temperature changes in the tissue underlying the fiberoptic light source and did not detect a significant change with the highest stimulation parameters used in this study (Figure S5).

Discussion

Here, we present a minimally invasive investigation of the functional hemodynamic response to direct cortical

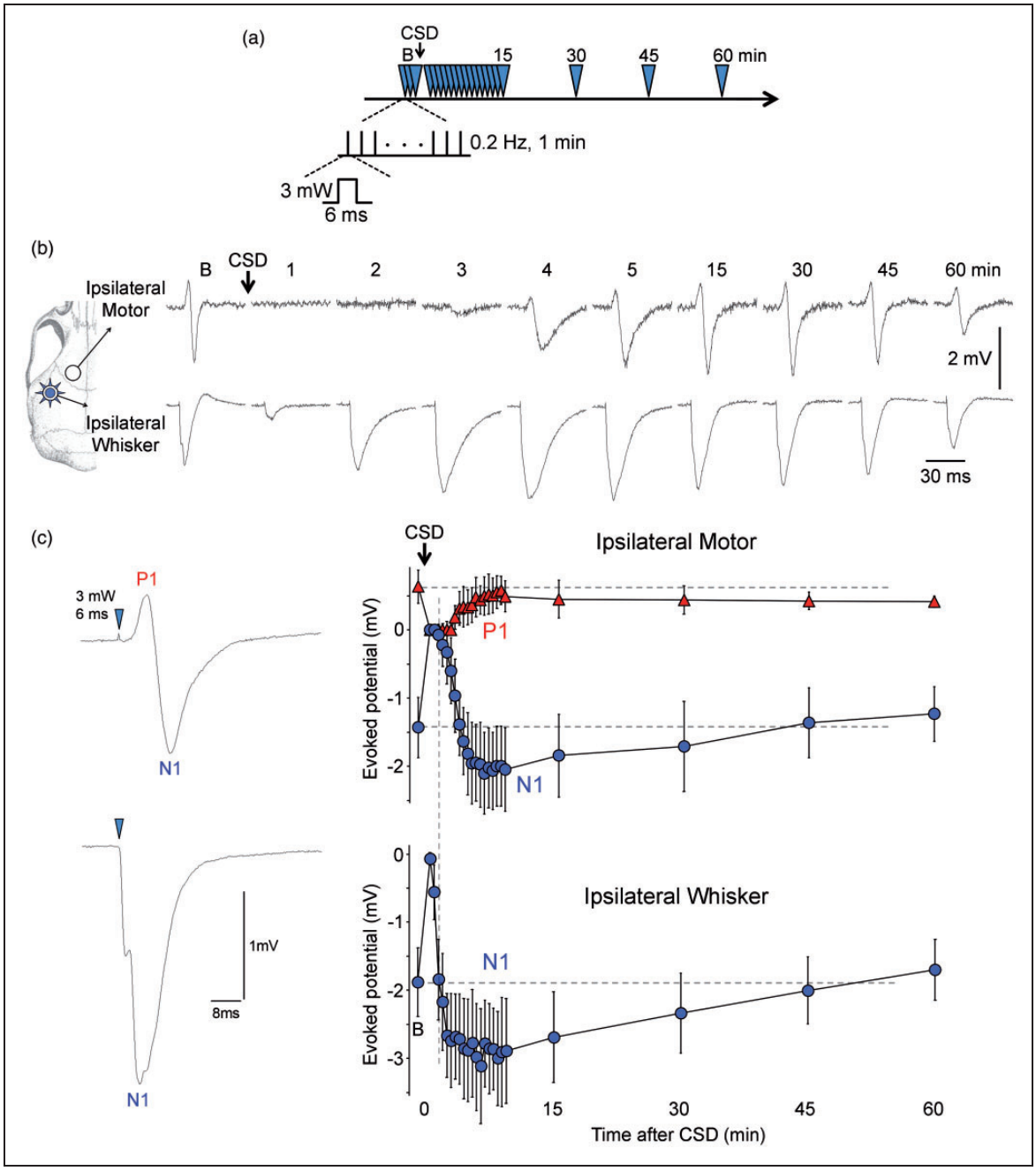

Figure 6. Effect of cortical spreading depression on optogenetic evoked potentials. (a) Timeline shows the stimulation protocol where optogenetic stimulation of whisker barrel cortex (3 mW, 0.2 Hz, 6 ms; blue arrowheads) was delivered at indicated time points to evoke field potentials in ipsilateral whisker and motor cortices. (b) Representative optogenetic evoked potentials in ipsilateral whisker and motor cortices before (b, baseline) and 1–60 min after CSD as indicated on each tracing. (c) Time course of optogenetic evoked potential amplitudes in ipsilateral whisker and motor cortices before (b, baseline) and after CSD ($p < 0.0001$, time factor; $n = 5$ mice; one-way ANOVA for repeated measures followed by Dunnett's multiple comparisons). Time 0 is CSD onset. Positive (P1) and negative (N1) peaks are measured and shown separately for motor cortex. Vertical dashed line indicates the time ipsilateral whisker evoked potentials recovered to baseline.

pyramidal neuron stimulation using optogenetics in ChR2 transgenic mice. We took a systematic approach to determine the spatiotemporal and dose-response characteristics of the CBF response. We stimulated the barrel cortex and imaged local and remote CBF responses over the entire dorsal cortex using LSF through intact skull, under full systemic physiological monitoring and maintenance. We observed robust focal

hyperemia within the stimulated whisker barrel cortex and within ipsilateral motor cortex, both of which were coupled to large amplitude epicranial evoked potentials. The responses were both pulse amplitude- and frequency- but not duration-dependent. The magnitude and time course of optogenetic hyperemia both in the whisker barrel cortex and in the remotely activated ipsilateral motor cortex closely resembled functional hyperemia in response to somatosensory activation.[26,27] Moreover, we detected a small but highly reproducible oligemia in contralateral hemisphere likely mediated by transcortical inhibition. Further supporting an overlap with physiological functional neurovascular coupling, neurovascular coupling during optogenetic activation was also suppressed by CSD. Altogether, the model provided a minimally invasive approach to examine both local and remote neurovascular coupling in response to excitatory and inhibitory inputs that can be employed to interrogate cerebrovascular function in disease models.

Previous studies employed optogenetic activation to evoke hemodynamic responses recorded by BOLD fMRI[28,29] or intrinsic optical signal (IOS) imaging.[11,12,30] However, neither BOLD nor IOS, which are effectively measures of blood volume, reflects the true CBF response. Two studies combined IOS with laser Doppler flowmetry,[30,31] which does not provide spatial information. Others have combined IOS with LSF,[32] but these studies used craniotomies, and thus were invasive, which can confound cerebrovascular physiology. Most studies did not monitor arterial blood pressure and pCO_2, or inadvertent CSD occurrence during experimental preparation, which are critical confounders of CBF response during functional activation. Therefore, our approach has distinct advantages over previous studies, including measurement of relative CBF rather than its surrogates, spatial information, and minimally invasive methodology with full systemic physiological monitoring.

The hyperemic responses in both whisker barrel and motor cortices were intensity-dependent. The power density range we employed (1–5 mW applied via 400 μm diameter fiber, ~8–40 mW/mm^2) was likely attenuated to some degree by the skull, meninges and subarachnoid space before reaching the cortical surface.[8,33] Thereafter, tissue scattering, absorption and conical spread (numerical aperture 0.39) lead to rapid attenuation at increasing depths (~1% of original power density within a ~0.5 mm radius from the source) based on prior work.[34] Consistent with these, the lowest power level we employed (1 mW, ~8 mW/mm^2 at skull surface) did not trigger significant hyperemia, whereas higher power levels likely reached ChR2 activation threshold in the tissue. We do not know with any degree of precision how far in the cortex the stimulus light reached at each power level, *in vivo*. However, layer I (i.e. molecular layer), where ChR2 is strongly expressed in this transgenic line,[14,15] was more likely to be activated at lower intensities, and cortical tissues deeper than 500 μm (i.e. layers V/VI) were less likely to be directly activated even at our highest intensity (~99% attenuation), despite the high expression of ChR2 in layer V pyramidal cells. Therefore, we believe our transcranial stimulation paradigm primarily depolarized layer I apical dendrites at lower intensities, and layer IV barrels at higher intensities.[35]

Because spike probability does not drop significantly at optogenetic stimulation frequencies lower than 30 Hz,[14,36] we did not see a ceiling effect across the 4–12 Hz range, consistent with previous data.[11,31] In contrast to previous work,[30,31] however, pulse duration did not significantly modulate the local hyperemic responses in the barrel cortex, where 2-ms pulses appeared almost as effective as 10 ms (3 mW, 8 Hz, 30-s train). Based on the response kinetics of ChR2, pulse duration of 2 ms is less likely to trigger neuronal spiking,[14,36] suggesting that depolarizations below the spike threshold may still be sufficient to evoke a local blood flow response. Lastly, given that the hyperemic response has already started to plateau by the end of our 30-s stimulus train, longer train durations would have been unlikely to yield larger hyperemic responses. We avoided further increasing the pulse intensity, frequency and duration, and stimulus train duration, in order to avoid depolarization block[37] or inadvertent CSD induction.[8]

There has been conflicting data on whether ionotropic glutamate receptor blockade inhibits local hyperemia to optogenetic stimulation[31,32]; the discrepancy may stem from the invasive nature of such studies or the optogenetic light directly affecting the laser Doppler flow signal. We did not attempt to pharmacologically dissect the mediators of optogenetic hyperemia mainly to avoid a craniectomy for drug applications and preserve the physiological state of the tissue. Instead, we tested whether CSD, known to disrupt physiological neurovascular coupling for more than an hour,[24] also inhibits optogenetic functional hyperemia. Indeed, CSD caused neurovascular uncoupling both in the optogenetically activated barrel cortex, and in the remote, synaptically activated motor cortex to a similar extent for at least an hour, suggesting that neurovascular coupling mechanisms during optogenetic cortical activation overlap to some extent with those during physiological somatosensory activation.

Our findings also reflect known functional connectivity among various cortical regions. We observed ipsilateral motor cortex hyperemia in response to whisker barrel cortex stimulation which was presumably evoked by well-known excitatory projections between the two

regions.[38] As such, the CBF response in the ipsilateral motor cortex represented a synaptically induced functional hyperemia. In contrast, contralateral barrel and motor cortices developed small but reproducible oligemic responses despite showing evoked potentials similar to the ipsilateral motor cortex. The contralateral barrel cortex evoked potentials were likely due to activation of transcallosal projections of layer II/III pyramidal neurons[39] that are known to mediate interhemispheric inhibition of layer V pyramidal neurons.[21,40,41] Therefore, the oligemic response was consistent with transcallosal inhibition, which we also demonstrated electrophysiologically using paired somatosensory-optogenetic stimulation. To our knowledge, such a decrease in CBF in the contralateral homotopic cortex after optogenetic stimulation has not been reported, although a subtle decrease in cerebral blood volume may have been detected when examined using IOS in a recent study.[11] More work is needed to determine whether contralateral oligemia is simply a neurovascular coupling response to reduced neuronal activity or directly induced by transcallosal projections and their targets.

Last but not the least, we carried out control experiments to eliminate potential confounders. While room light did not cause ChR2 activation, surgical microscope light induced a small CBF increase and, therefore, was kept off for all recordings. Wild type ($ChR2^-$) mice did not respond to optogenetic stimulation, confirming specificity of responses in $ChR2^+$. Optogenetic stimulation used in this study did not significantly change tissue temperature. We also monitored for inadvertent CSD induction that can occur during optogenetic stimulation,[8] which profoundly alters resting CBF, impairs neurovascular coupling,[24] and induces lasting changes in evoked electrophysiological activity as we have demonstrated in this study.

The optogenetic approach, of course, has several disadvantages: (a) The precise mechanisms of neurovascular coupling during optogenetic stimulation may differ from coupling during physiological activation (e.g. upon somatosensory stimulation); (b) the non-invasive approach requires transgenic mice; (c) transgene expression shows regional heterogeneity[8]; therefore, identical regions must be studied in different animals and cohorts for comparisons; (d) excess stimulation can lead to silencing of neurons due to depolarization block,[37] and, at its extreme, cause heat- and light-induced injury[8]; and (e) the non-invasive method is limited to interrogation of the dorsal cortex.

In conclusion, our data suggest that optogenetic functional hyperemia, as a model for neurovascular coupling, displays overlap with physiological (e.g. somatosensory-induced) functional hyperemia, and can be employed in combination with optical imaging to examine CBF dynamics. We envision that the optogenetic approach can be modified for longitudinal studies in the same animal over time to examine, for example, the impact of brain injury, neurodegeneration or cerebrovascular dysfunction on neurovascular coupling.

Funding

The author(s) disclosed receipt of the following financial support for the research, authorship, and/or publication of this article: This work was supported by the NIH (P01NS055104, R01NS102969 and R25NS065743), the Foundation Leducq, the Heitman Foundation, the Ellison Foundation, the Brain Aneurysm Foundation's Timothy P. Susco and Andrew David Heitman Foundation Chairs of Research, the Aneurysm and AVM Foundation, the Lawrence M. Brass Stroke Research Award from the American Heart Association and American Brain Foundation (18POST34030369), and by a fellowship from the Boehringer Ingelheim Fonds.

Declaration of conflicting interests

The author(s) declared no potential conflicts of interest with respect to the research, authorship, and/or publication of this article.

Authors' contributions

MB, DYC, CAG, TQ, TT, HS, KS conducted the experiments, analyzed the data, and helped draft the manuscript; SS and MAY contributed to data analysis, data interpretation and manuscript preparation; CA conceived and designed the study, analyzed and interpreted the data, and prepared the manuscript.

Supplementary material

Supplemental material for this article is available online.

ORCID iD

David Y Chung https://orcid.org/0000-0002-7149-5851

References

1. Kisler K, Nelson AR, Montagne A, et al. Cerebral blood flow regulation and neurovascular dysfunction in Alzheimer disease. *Nat Rev Neurosci* 2017; 18: 419–434.
2. Koide M, Bonev AD, Nelson MT, et al. Inversion of neurovascular coupling by subarachnoid blood depends on large-conductance Ca2+-activated K+ (BK) channels. *Proc Natl Acad Sci U S A* 2012; 109: E1387–E1395.
3. Shin HK, Jones PB, Garcia-Alloza M, et al. Age-dependent cerebrovascular dysfunction in a transgenic mouse model of cerebral amyloid angiopathy. *Brain* 2007; 130(Pt 9): 2310–2319.
4. Capone C, Dabertrand F, Baron-Menguy C, et al. Mechanistic insights into a TIMP3-sensitive pathway constitutively engaged in the regulation of cerebral hemodynamics. *Elife* 2016; 5: e17536.

5. Capone C, Cognat E, Ghezali L, et al. Reducing Timp3 or vitronectin ameliorates disease manifestations in CADASIL mice. *Ann Neurol* 2016; 79: 387–403.
6. Toth P, Szarka N, Farkas E, et al. Traumatic brain injury-induced autoregulatory dysfunction and spreading depression-related neurovascular uncoupling: pathomechanism and therapeutic implications. *Am J Physiol Heart Circ Physiol* 2016; 311: H1118–H1131.
7. Iadecola C. The neurovascular unit coming of age: a journey through neurovascular coupling in health and disease. *Neuron* 2017; 96: 17–42.
8. Chung DY, Sadeghian H, Qin T, et al. Determinants of optogenetic cortical spreading depolarizations. *Cereb Cortex* 2019; 29: 1150–1161.
9. Christie IN, Wells JA, Kasparov S, et al. Volumetric spatial correlations of neurovascular coupling studied using single pulse opto-fMRI. *Sci Rep* 2017; 7: 41583.
10. Uhlirova H, Kilic K, Tian P, et al. Cell type specificity of neurovascular coupling in cerebral cortex. *Elife* 2016; 5: pii:e14315.
11. Bauer AQ, Kraft AW, Baxter GA, et al. Effective connectivity measured using optogenetically evoked hemodynamic signals exhibits topography distinct from resting state functional connectivity in the mouse. *Cereb Cortex* 2018; 28: 370–386.
12. Pisauro MA, Dhruv NT, Carandini M, et al. Fast hemodynamic responses in the visual cortex of the awake mouse. *J Neurosci* 2013; 33: 18343–18351.
13. Lee JH, Durand R, Gradinaru V, et al. Global and local fMRI signals driven by neurons defined optogenetically by type and wiring. *Nature* 2010; 465: 788–792.
14. Wang H, Peca J, Matsuzaki M, et al. High-speed mapping of synaptic connectivity using photostimulation in Channelrhodopsin-2 transgenic mice. *Proc Natl Acad Sci U S A* 2007; 104: 8143–8148.
15. Arenkiel BR, Peca J, Davison IG, et al. In vivo light-induced activation of neural circuitry in transgenic mice expressing channelrhodopsin-2. *Neuron* 2007; 54: 205–218.
16. Ayata C, Dunn AK, Gursoy OY, et al. Laser speckle flowmetry for the study of cerebrovascular physiology in normal and ischemic mouse cortex. *J Cereb Blood Flow Metab* 2004; 24: 744–755.
17. Franklin K and Paxinos G. *The mouse brain in stereotaxic coordinate*, 3rd edn. San Diego: Academic Press, 2008.
18. Zakiewicz IM, Bjaalie JG and Leergaard TB. Brain-wide map of efferent projections from rat barrel cortex. *Front Neuroinform* 2014; 8: 5.
19. Petersen CC. The functional organization of the barrel cortex. *Neuron* 2007; 56: 339–355.
20. Devor A, Hillman EM, Tian P, et al. Stimulus-induced changes in blood flow and 2-deoxyglucose uptake dissociate in ipsilateral somatosensory cortex. *J Neurosci* 2008; 28: 14347–1457.
21. Palmer LM, Schulz JM, Murphy SC, et al. The cellular basis of GABA(B)-mediated interhemispheric inhibition. *Science* 2012; 335: 989–993.
22. Straub SV and Nelson MT. Astrocytic calcium signaling: the information currency coupling neuronal activity to the cerebral microcirculation. *Trends Cardiovasc Med* 2007; 17: 183–190.
23. Attwell D, Buchan AM, Charpak S, et al. Glial and neuronal control of brain blood flow. *Nature* 2010; 468: 232–243.
24. Ayata C and Lauritzen M. Spreading depression, spreading depolarizations, and the cerebral vasculature. *Physiol Rev* 2015; 95: 953–993.
25. Christie IN, Wells JA, Southern P, et al. fMRI response to blue light delivery in the naive brain: implications for combined optogenetic fMRI studies. *Neuroimage* 2013; 66: 634–641.
26. Ma J, Ayata C, Huang PL, et al. Regional cerebral blood flow response to vibrissal stimulation in mice lacking type I NOS gene expression. *Am J Physiol* 1996; 270(3 Pt 2): H1085–H1090.
27. Ayata C, Ma J, Meng W, et al. L-NA-sensitive rCBF augmentation during vibrissal stimulation in type III nitric oxide synthase mutant mice. *J Cereb Blood Flow Metab* 1996; 16: 539–541.
28. Kahn I, Desai M, Knoblich U, et al. Characterization of the functional MRI response temporal linearity via optical control of neocortical pyramidal neurons. *J Neurosci* 2011; 31: 15086–15091.
29. Desai M, Kahn I, Knoblich U, et al. Mapping brain networks in awake mice using combined optical neural control and fMRI. *J Neurophysiol* 2011; 105: 1393–1405.
30. Vazquez AL, Fukuda M, Crowley JC, et al. Neural and hemodynamic responses elicited by forelimb- and photostimulation in channelrhodopsin-2 mice: insights into the hemodynamic point spread function. *Cereb Cortex* 2014; 24: 2908–2919.
31. Iordanova B, Vazquez AL, Poplawsky AJ, et al. Neural and hemodynamic responses to optogenetic and sensory stimulation in the rat somatosensory cortex. *J Cereb Blood Flow Metab* 2015; 35: 922–932.
32. Scott NA and Murphy TH. Hemodynamic responses evoked by neuronal stimulation via channelrhodopsin-2 can be independent of intracortical glutamatergic synaptic transmission. *PLoS One* 2012; 7: e29859.
33. Yizhar O, Fenno LE, Davidson TJ, et al. Optogenetics in neural systems. *Neuron* 2011; 71: 9–34.
34. Aravanis AM, Wang LP, Zhang F, et al. An optical neural interface: in vivo control of rodent motor cortex with integrated fiberoptic and optogenetic technology. *J Neural Eng* 2007; 4: S143–S156.
35. Cardin JA, Carlen M, Meletis K, et al. Targeted optogenetic stimulation and recording of neurons in vivo using cell-type-specific expression of Channelrhodopsin-2. *Nat Protoc* 2010; 5: 247–254.
36. Boyden ES, Zhang F, Bamberg E, et al. Millisecond-timescale, genetically targeted optical control of neural activity. *Nat Neurosci* 2005; 8: 1263–1268.
37. Herman AM, Huang L, Murphey DK, et al. Cell type-specific and time-dependent light exposure contribute to

silencing in neurons expressing Channelrhodopsin-2. *Elife* 2014; 3: e01481.
38. Fabri M and Burton H. Ipsilateral cortical connections of primary somatic sensory cortex in rats. *J Comp Neurol* 1991; 311: 405–424.
39. Fame RM, MacDonald JL and Macklis JD. Development, specification, and diversity of callosal projection neurons. *Trends Neurosci* 2011; 34: 41–50.
40. Asanuma H and Okuda O. Effects of transcallosal volleys on pyramidal tract cell activity of cat. *J Neurophysiol* 1962; 25: 198–208.
41. Ferbert A, Priori A, Rothwell JC, et al. Interhemispheric inhibition of the human motor cortex. *J Physiol* 1992; 453: 525–546.